Biochemical and Biophysical Research Communications 456 (2015) 35–40

Contents lists available at ScienceDirect

Biochemical and Biophysical Research Communications

journal homepage: www.elsevier.com/locate/ybbrc

Crystal structure of 5-formyl-3-hydroxy-2-methylpyridine 4-carboxylic acid 5-dehydrogenase, an NAD$^+$-dependent dismutase from *Mesorhizobium loti*

Andrew Njagi Mugo [a], Jun Kobayashi [b], Bunzo Mikami [b], Yu Yoshikane [c], Toshiharu Yagi [c], Kouhei Ohnishi [a,*]

[a] Research Institute of Molecular Genetics, Kochi University, Nankoku, Kochi 783-8502, Japan
[b] Division of Applied Life Sciences, Graduate School of Agriculture, Kyoto University, Gokasho, Uji, Kyoto 611-0011, Japan
[c] Faculty of Agriculture and Agricultural Science Program, Graduate School of Integrated Arts and Science, Kochi University, Nankoku, Kochi 783-8502, Japan

ARTICLE INFO

Article history:
Received 27 October 2014
Available online 18 November 2014

Keywords:
5-Formyl-3-hydroxy-2-methylpyridine 4-carboxylic acid 5-dehydrogenase
3-Hydroxyacyl-CoA dehydrogenase
Mesorhizobium loti
Vitamin B_6-degradation pathway
Dismutase
Nicotinamide adenine dinucleotide

ABSTRACT

5-Formyl-3-hydroxy-2-methylpyridine 4-carboxylic acid 5-dehydrogenase (FHMPCDH) from *Mesorhizobium loti* is the fifth enzyme in degradation pathway I for pyridoxine. The enzyme catalyzes a dismutation reaction: the oxidation of 5-formyl-3-hydroxy-2-methylpyridine 4-carboxylic acid (FHMPC) to 3-hydroxy-2-methylpyridine 4,5-dicarboxylic acid with NAD$^+$ and reduction of FHMPC to 4-pyridoxic acid with NADH. FHMPCDH belongs to the L-3-hydroxyacyl-CoA dehydrogenase (HAD) family. The crystal structure was determined by molecular replacement and refined to a resolution of 1.55 Å (R-factor of 16.4%, R_{free} = 19.4%). There were two monomers in the asymmetric unit. The overall structure of the monomer consisted of N- and C-terminal domains connected by a short linker loop. The monomer was similar to members of the HAD family (RMSD = 1.9 Å). The active site was located between the domains and highly conserved to that of human heart L-3-hydroxyacyl-CoA dehydrogenase (HhHAD). His-Glu catalytic dyad, a serine and two asparagine residues of HhHAD were conserved. Ser116, His137 and Glu149 in FHMPCDH are connected by a hydrogen bonding network forming a catalytic triad. The functions of the active site residues in the reaction mechanism are discussed.

1. Introduction

5-Formyl-3-hydroxy-2-methylpyridine 4-carboxylic acid 5-dehydrogenase (FHMPCDH) participates in degradation pathway I for pyridoxine, a free form of vitamin B_6 [1,2]. The genes encoding the enzymes of pathway I occur as a cluster in chromosomal DNA of *Mesorhizobium loti* MAFF303099, a nitrogen-fixing symbiotic bacterium [3]. FHMPCDH is the fifth enzyme in the pathway and is encoded by the gene *mlr6793* [4]. FHMPCDH catalyzes the oxidation of 5-formyl-3-hydroxy-2-methylpyridine 4-carboxylic acid (FHMPC) to 3-hydroxy-2-methylpyridine 4,5-dicarboxylic acid (HMPDC) with NAD$^+$ and the reduction of FHMPC to 4-pyridoxic acid with NADH as a hydrogen donor [4,5] as shown below.

Abbreviations: DKR, diketoreductase; DTT, dithiothreitol; FHMPC, 5-formyl-3-hydroxy-2-methylpyridine 4-carboxylic acid; FHMPCDH, 5-formyl-3-hydroxy-2-methylpyridine 4-carboxylic acid 5-dehydrogenase; HAD, 3-hydroxyacyl-CoA dehydrogenase; HBDH, (*S*)-3-hydroxybutyryl-CoA dehydrogenase; HhHAD, human heart L-3-hydroxyacyl-CoA dehydrogenase; HMPDC, 3-hydroxy-2-methylpyridine 4,5-dicarboxylic acid; 4-PADH, 4-pyridoxic acid dehydrogenase; RGHD, rabbit L-gulonate 3-dehydrogenase.

* Corresponding author. Fax: +81 88 864 5109.
E-mail address: kouheio@kochi-u.ac.jp (K. Ohnishi).

http://dx.doi.org/10.1016/j.bbrc.2014.11.028
0006-291X/

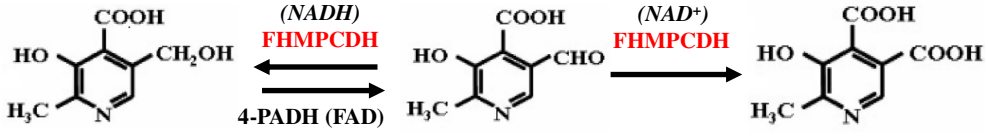

4-Pyridoxic acid

5-Formyl-3-hydroxy-2-methyl pyridine-4-carboxylic acid

3-Hydroxy-2-methylpyridine-4,5-dicarboxylic acid

FHMPCDH has been purified and characterized from two bacteria, *Pseudomonas* MA-1 and *M. loti* [4,5].The enzyme is a homodimer with subunit molecular mass of 34 kDa. FHMPCDH belongs to the L-3-hydroxyacyl-CoA dehydrogenase (HAD) family because its 181–206 residues correspond to the PROSITE motif of HAD (Supplemental Fig. 1). However, FHMPCDH also contains the signature sequence of 3-hydroxyisobutyrate dehydrogenase at residues 7–20. A consensus sequence, HXFXPX$_3$MXLXE, has been identified as the signature of the HAD family [6]; however, in FHMPCDH only three residues of the consensus sequence **H**XXX**P**X$_3$XXXX**E** are conserved. HADs have been found in mitochondria and peroxisomes of different species [7–9]. The crystal structures of HAD from pig [10], *Caenorhabditis elegans* [11] and human [12] have been solved and the catalytic mechanism of human heart HAD has been proposed [13]. FHMPCDH shares 32% identity with human heart 3-hydroxyacyl-CoA dehydrogenase (HhHAD). HAD catalyzes oxidation of the hydroxyl group of L-3-hydroxyacyl CoA to a keto group. A conserved His-Glu dyad is vital for HAD catalytic mechanism. The His residue acts as a catalytic/general base [11–16]. In HhHAD, His158 has been proposed as the catalytic base and Glu170 is involved in proper orientation of the His residue. Our previous report shows that His137 and Glu149 correspond to a His-Glu pair [4]. FHMPCDH also shares 30% identity with rabbit L-gulonate 3-dehydrogenase (RGHD), an NAD^+ dependent enzyme in the uronate cycle that catalyzes oxidation of L-gulonate to 3-dehydro-L-gulonate [17]; and 30% identity with diketoreductase (DKR), an enzyme that catalyzes the two-step bioreduction on the dicarbonyl substrate [18,19]. These enzymes also contain a His-Glu pair. The crystal structures of these enzymes show that the active site architecture is highly conserved. In addition to the His-Glu pair, a conserved serine and two asparagine residues are localized in the active site of all the structures.

FHMPCDH is also a dismutase [4,5]. The enzyme catalyzes the oxidation and reduction of FHMPC at the same rate with NAD^+ or NADH. Liver alcohol dehydrogenase of horse [20] and human [21] show the dismutation reaction of aldehydes. In contrast to the alcohol dehydrogenases, FHMPCDH shows an unmeasurable oxidation activity towards the corresponding alcohol (4-pyridoxic acid) in the presence of NAD^+ (a reverse reaction of reduction of FHMPC) [4]. The dismutase activities of the other HAD family enzymes are not reported.

Here, we examined the tertiary structure of FHMPCDH to elucidate the catalytic mechanism of the enzyme. The interaction of the active site residues will give a clue to the mechanism of the dismutation activity of the enzyme. It was found that the over-all structure of the subunit and the arrangement of the active site residues are similar to those of HhHAD.

2. Materials and methods

2.1. Overexpression and purification of enzyme and enzyme assays

FHMPCDH was overexpressed in *Escherichia coli* as described previously [4] with slight modification. The enzyme was homogeneously purified by QA52 and Blue A column chromatography, with 1 mM DTT added to all buffers. The purified enzyme was thoroughly dialyzed at 4 °C against the crystallization buffer (50 mM Tris–HCl (pH 8.0), 10% (w/v) glycerol, 1 mM DTT and 0.01% (v/v) 2-mercaptoethanol).

FHMPCDH activity was determined by following the initial decrease in A_{380} (ε: 1000 M^{-1} cm^{-1}) due to FHMPC consumed at 30 °C in 1 ml of a reaction mixture consisting of 0.1 M sodium phosphate, pH 8.0, 0.5 mM FHMPC, 0.5 mM NAD^+ and an appropriate amount of the enzyme [4]. Protein concentration was measured by the protein–dye method [22] during purification and the protein concentration of FHMPCDH was determined from the molar absorption coefficient (ε280 = 21,430 cm^{-1} M^{-1}) for purity.

2.2. Crystallization

Crystallization was done by the sitting drop vapor diffusion method. A mixture consisting of 2 μl of enzyme solution in crystallization buffer and 2 μl of reservoir solution was equilibrated against 100 μl of reservoir solution at 277 K. Low-quality crystals grew after 1 week with reservoir solution No. 11 (0.2 M NH_4-acetate, 0.1 M Na-acetate (pH 4.6) and 30% PEG 4000) from the Crystallization Basic Kit for Proteins. The condition was optimized to 0.2 M NH_4-acetate, 0.1 M Na-acetate (pH 6.5) and 30% PEG 4000. Good quality crystals grew within 3 weeks.

2.3. X-ray data collection and structure determination

X-ray diffraction data were collected at the BL26B1 station of SPring-8 (Hyogo, Japan). The initial phase was determined by the molecular replacement method using the MOLREP program [23] in the CCP4 program suite [24] with the structure of L-3-hydroxyacyl CoA dehydrogenase (PDB ID: 1F12) as a search model. The structure was refined to a resolution of 1.55 Å by refinement with REFMAC5 [25] and PHENIX [27] and manual model building by COOT [26]. The quality of the structure factor and the final model was checked using the PROCHECK [28] and SFCHECK [29] programs. The refined model and structure factors were deposited in the Protein Data Bank with accession code 4OM8.

3. Results and discussion

3.1. Amino acid sequence comparison with other enzymes

To find candidate proteins for molecular replacement, a similarity search using an amino acid sequence of FHMPCDH was done. FHMPCDH showed significant similarity to those of the HAD family. In addition, FHMPCDH also showed identity to those of DKR, a member of dicarbonyl reductases [30], and RGHD, a member of the GDH/γCRY family [31] as described below. The three sequences highly homologous to that of FHMPCDH are aligned in Supplemental Fig. 1. The sequence alignment showed the catalytic His-Glu pair together with Ser and Asn residues correspond to His137, Glu149, Ser116, Asn188 and Asn140 in FHMPCDH. The distribution of secondary structure elements in FHMPCDH was similar to that in HhHAD [12]. However, HhHAD had an extra helix in the N-terminus domain (residues 74–86) that was not found in FHMPCDH. In contrast, FHMPCDH had an extra helix in the C-terminus domain (α-11, residues 283–306).

Table 1
Data collection and refinement statistics for FHMPCDH.

Data collection	
X-ray source	SPring-8 BL26B1
Wavelength (Å)	0.800
Detector	Saturn A200
Space group	*C2*
Unit-cell length (Å)	a = 122.81, b = 44.21, c = 109.34
Unit-cell angle (°)	90.00, 116.35, 90.00
Processing software	HKL-2000
Resolution limit (Å)	50.00–1.55 (1.58–1.55)
Measured reflections	437,317 (534)
Unique reflections	75,976 (3734)
Completeness (%)	96.2 (87.4)
Redundancy	5.8 (5.5)
$\langle I\rangle/\langle\sigma(I)\rangle$	17.1 (2.6)
Refinement	
Resolution (Å)	27.34–1.55 (1.57–1.55)
Used reflections	75,969 (2534)
Rwork (%)	16.4 (17.84)
Rfree (%)	19.4 (23.74)
Residue/Wat/NAD$^+$	309/679/1
Average B factor (Å^2)	18.0
RMS bond (Å)	0.007
RMS angle (°)	1.173
RMS chirality (°)	0.046
RMS planarity (Å)	0.006
RMS dihedral (°)	15.40
Residue in favored region (%)	97.5
Residue in allowed region (%)	2.3
Coordinate error (Å)	0.14

Values in parentheses are for the outermost shell at the section of data collection.

3.2. Overall structure

The structure of FHMPCDH was determined and refined to a resolution of 1.55 Å (Table 1). The structure contains two monomers in the asymmetric unit (Fig. 1A and Supplemental Fig. S2), which is in good agreement with FHMPCDH existing as a homodimer in solution [4]. PISA analysis shows that subunit A and B form a dimer with total buried surface area of 10,440 Å and 10,360 Å, respectively. The monomeric structure of FHMPCDH consisted of the N- and C-terminal domains (Fig. 1B). The N-terminal domain (residues 1–178) consists of eight β-strands (β1–β8), six α-helixes (α1–α5 and α7) and a 3_{10}-helix (α6). The first six β-strands (β1–β6) are in parallel orientation and are sandwiched by six α-helixes. The last two-strands (β7–β8) are also parallel but run in the opposite direction relative to the first six strands (Fig. 1B). The C-terminal domain (residues 186–309) adopts an entirely helical architecture. It consists of four α-helixes (α8–α11). In contrast to other straight helixes, helix α9 contains several turns: α-turn, between Ile224 and Gly228; γ-turn, between Pro229 and Ala231; β-turn, between Met230 and Leu233; β-turn, between Leu232 and Met235; and α-turn between Leu233 and Gly237. Thus α-helix9 protrudes to the solvent. The three highly conserved aspartic and glycine residues (Asp213, Asp234, Asp239, Gly219, Gly221, Gly228 and Gly237) are located in helix α9 [11,12]. The two domains are connected by a short linker loop made of residues 179–185, in which Pro183, Gly184 and Phe185 make the conserved PGF sequence found in the HAD family. The putative active site is located between the two domains (Fig. 1C).

A DALI search [32] using the monomer structure of FHMPCDH shows high similarity to RGHD [31], followed by diketoreductase [19] and (*S*)-3-hydroxybutyryl-CoA dehydrogenase (HBDH) from *Clostridium butyricum* [33] (Supplemental Table S1). The major difference was on the C-terminal domain: FHMPCDH contains an extra helix in the C-terminal domain (α11) (Supplemental Fig. S3). When the DALI search was subjected to the N-terminal domain of FHMPCDH, the structure was most similar to that of HAD from *C. elegans* [11], followed by those of HBDH and

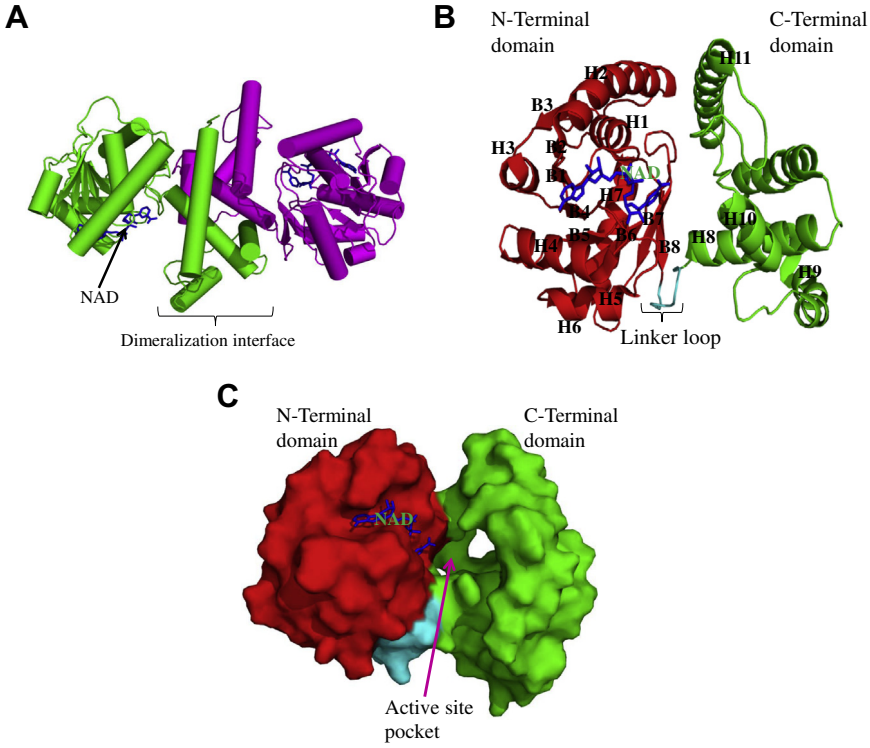

Fig. 1. Tertiary structure of FHMPCDH. (A) Overall shape of FHMPCDH dimer generated by symmetry operation. The two subunits are shown in green and magenta respectively. Each subunit contains bound NAD$^+$ shown as a stick in blue. (B) Tertiary structure of one subunit, the N-terminal, C-terminal domains and linker loop are colored red, green and cyan, respectively. NAD is shown as a stick in blue. Secondary structure elements, α-helix and β-sheet, are shown as H and B, respectively. N-terminus domain contains α-helix and β-sheet, C-terminal domain contains only α-helixes. (C) Surface structure of one monomer, the arrow shows the location of putative active site pocket. The colors of Fig. C are the same as those of Fig. B. (For interpretation of the references to color in this figure legend, the reader is referred to the web version of this article.)

multifunctional enzyme, type-1 [34]. The C-terminal domain showed low similarity to that of rabbit L-gulonate 3-dehydrogenase, HAD from *C. elegans* and HBDH (Table S1).

Proteins belonging to HAD and DKR utilize bulky substrates (4–16 carbons long), which are bound, extending from the N-terminal domain to the C-terminal domain in their active sites. The absence of an extra helix in the C-terminal domain may be to create space for the bulky substrates. In contrast, FHMPCDH utilizes smaller substrates [4] and can accommodate the extra helix.

3.3. Co-factor binding

The crystallized enzyme contained one molecule of NAD^+ per subunit. The NAD^+ was bound in an extended conformation in a cleft within the N-terminal domain with the adenine and nicotinamide rings oriented perpendicular to the planes of the corresponding riboses (Supplemental Fig. S4). NAD^+ is anchored by several hydrogen-bonding interactions between surrounding residues and water molecules (Fig. 2A). The residues and the distances involved are tabulated in Supplemental Table S2. In brief, the nicotinamide ring forms two hydrogen bonds with wat509 and wat574. The hydroxyl group of nicotinamide ribose receives hydrogen bonds from Glu89$O^{\varepsilon 2}$, Lys94 N^{ζ} and peptide forming oxygen of Val87. The pyrophosphate group forms hydrogen bonds with wat537, wat593, wat729 and wat863, and the peptide bond-forming nitrogen of Thr12 and Met13. The adenine ring of NAD^+ is anchored in place by hydrogen bonding with peptide bond-forming nitrogen of Val33 and wat763 and adenosine hydroxyl groups interact with $O^{\delta 1}$ and $O^{\delta 2}$ of Asp32, wat540 and wat731.

3.4. Dimerization interface

Subunit dimerization is mediated by 56 interactions between the residues in the C-terminal domains of the two subunits. The helixes of one subunit in the C-terminal domain run nearly antiparallel to the helixes of the other subunit: α8 and α8′, α11 and α11′, and part of α9 and α9′ (Supplemental Fig. S5). The dimer interface between α8 and α8′ is mediated by two pairs of salt bridges between Arg189 on one subunit and Glu197 on the other subunit. This Arg/Glu pair is conserved in the HAD family [11]. The dimer interface between α9 andα9′ is mediated by 12 hydrogen bonds (Asp213–Ala231/Met230, Ser217–Ile224, and Asp234–Ile273/Phe280) and the α11-α11′ pair is mediated by four hydrogen bonds (Lys297–leu305). All the residues that interact between the two subunits are summarized in Supplementary Table S3.

3.5. The interaction of the active site residues

The whole structures of FHMPCDH and HhHAD, which was used for molecular replacement, were superimposed (Supplemental

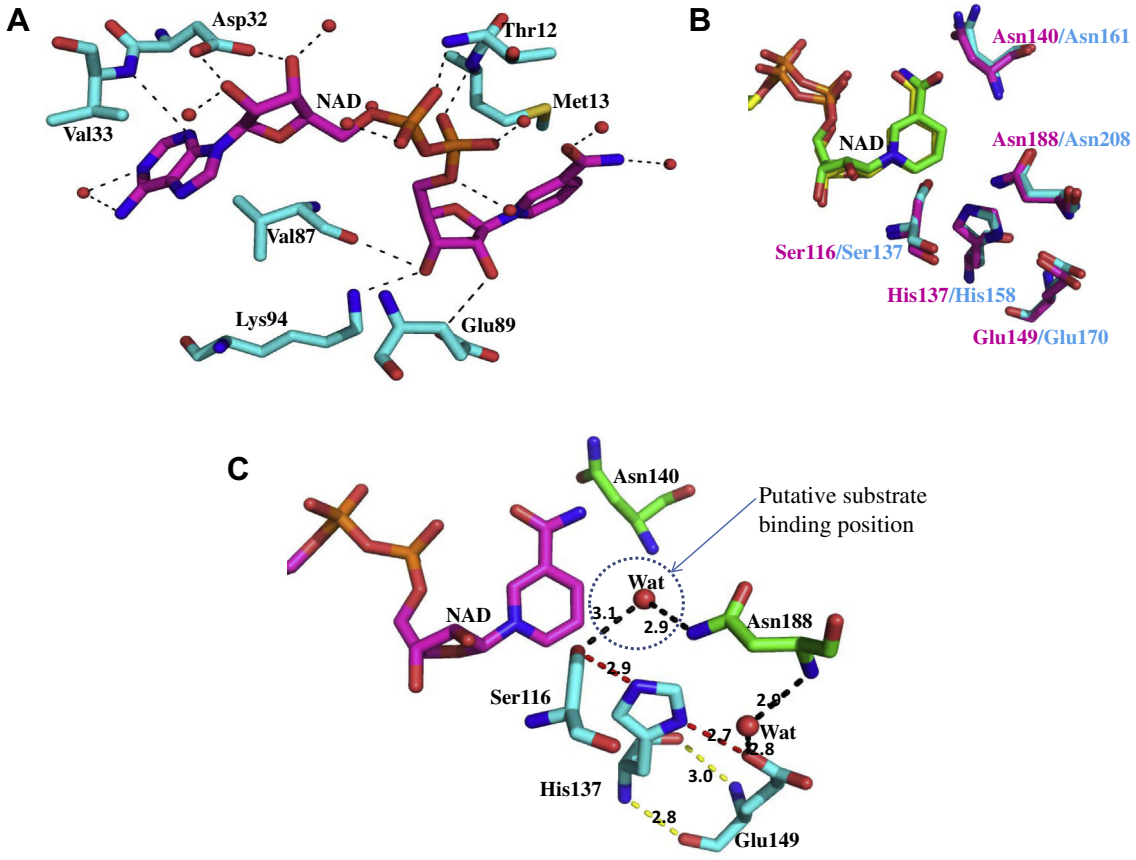

Fig. 2. The NAD^+ binding mode and the active site of FHMPCDH. (A) The residues and water molecules involved in NAD^+ binding. Carbon atoms of NAD^+ are in magenta; carbon atom of amino acids residues, cyan; oxygen, red; nitrogen, blue; and phosphate, orange. Water molecules are shown as red spheres. The hydrogen bonds are shown as black dotted lines. (B) Stereo view of the superimposed active sites of FHMPCDH and HhHAD. Carbons of residues in FHMPCDH and HhHAD are shown in magenta and cyan, respectively. Carbons of NAD molecules in FHMPCDH and HhHAD are shown in yellow and green, respectively. Nitrogen, oxygen, and phosphorus are shown in blue, red, and orange, respectively. (C) The interactions of the active site residues. Atoms are colored as follows: cyan, carbons of Ser116, His137 and Glu149 (catalytic triad, see text); green, carbons of Asn140 and Asn188; magenta, carbons of the NAD molecule; red, oxygen; blue, nitrogen; and orange, phosphate. Water molecules are shown as red spheres. Hydrogen bonds are shown as yellow dotted lines; the interactions of the catalytic triad are shown in red dotted lines. The interactions of Asn188 with the catalytic triad through water molecules are shown in black dotted lines. The distances between atoms are shown in Å. (For interpretation of the references to color in this figure legend, the reader is referred to the web version of this article.)

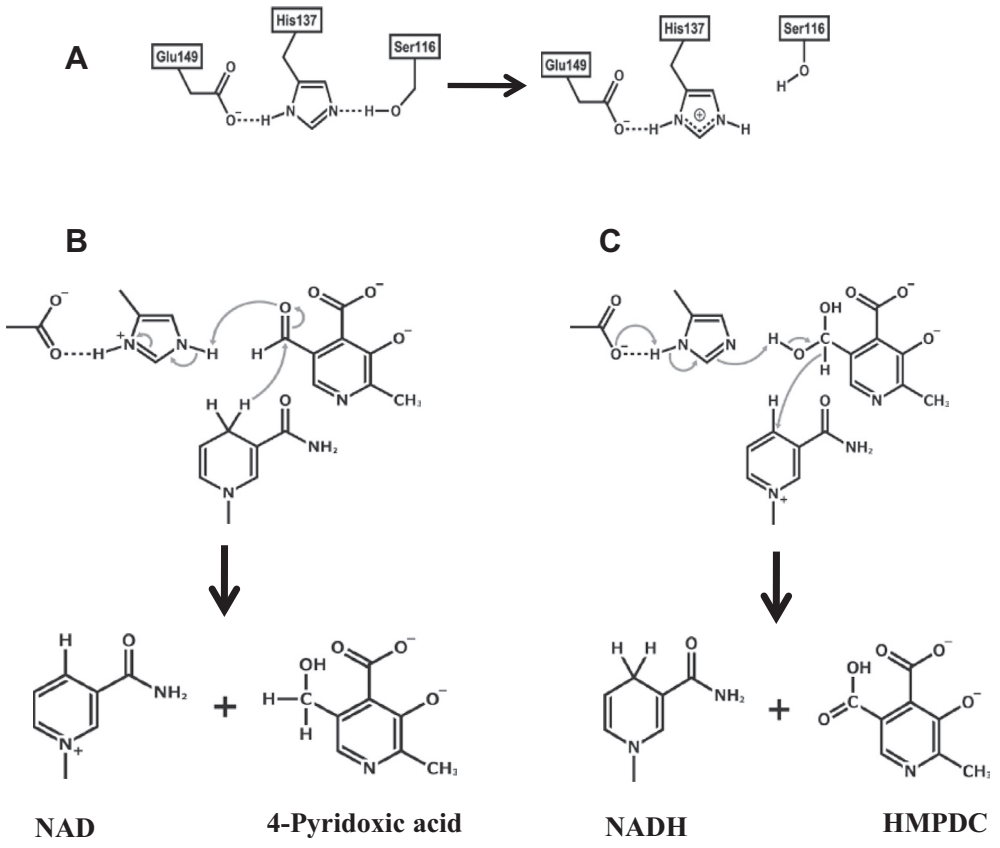

Fig. 3. The deduced reaction mechanism. (A) Catalytic triad formed by ser116, His137 and Glu149 and protonation of His137 by Ser116. (B) Reduction of FHMPC to 4-pyridoxic acid with NADH. (C) Oxidation of hemiacetal form of FHMPC with NAD^+ producing HMPDC and NADH.

Fig. S3). The extra helix in FDMPCDH is located between the N-terminal and C-terminal domains. The catalytic and substrate-binding residues (His137, Glu149, Ser116, Asn188 and Asn146) in FHMPCDH occupy almost the same positions as those (His158, Glu170, Ser137 Asn208 and Asn161) in HhHAD (Fig. 2B).

A His-Glu catalytic dyad together with a Ser residue has been proposed as important in the catalysis of HhHAD, DKR and RGDH which share high homology with FHMPCDH. In FHMPCDH, $N^{\delta 1}$ and $N^{\delta 2}$ of His137 are within hydrogen bonding distance to O^{ε} of Glu149 (2.7 Å) and O^{δ} of Ser116 (2.9 Å), respectively (Fig. 2C). The peptide bond-forming nitrogen and oxygen of His137 form a hydrogen bond with peptide bond-forming oxygen and nitrogen of Glu149, respectively. Thus, Ser116, His137 and Glu149 are connected by a hydrogen bonding network to form the catalytic triad. Asn188 may be involved in substrate-binding and stabilization of the bound substrate during the catalysis, because it is located at the same position as Asn208 in HhHAD.

The amide N of Asn188 and O^{ε} of Glu149 are within hydrogen bond distance (2.9 Å and 2.8 Å, respectively) to wat501. The water is located in the same position as one which is conserved in HAD enzymes and plays an important structural role (16). O^{γ} of ser116 and N^{δ} of Asn188 are also within hydrogen bond distance to wat543 at 3.1 Å and 2.9 Å, respectively (Fig. 2C).

3.6. Catalytic mechanism

FHMPCDH catalyzes oxidation of the hemiacetal form of FHMPC to HMPDC with NAD^+ and reduction of an aldehyde form of FHMPC to 4-pyridoxic acid with NADH. The Ser-His-Glu catalytic triad facilitates the two-way reactions. Ser116 assists protonation of His137 to drive the reduction reaction (Fig. 3A and B). His137 acts as a catalytic base to abstract a proton during oxidation (Fig. 3C). Glu149 likely neutralizes the positive charge on His137 after the deprotonation of the substrate.

The presence of Glu149 and Ser116 is necessary to drive the reaction at pH 8.0: the optimum pH of FHMPCDH. Glu149 donates electrons to drive the oxidation reaction. In our previous report, the E149Q mutant enzyme could not catalyze oxidation of FHMPC with NAD at pH 5.0 because the protonated imidazole was not able to donate electrons to drive the oxidation reaction without the donation of electrons from Glu149 [4]. In contrast, the E149Q mutant enzyme showed 148% higher K_{cat} value than the wild type for the reduction of FHMPC with NADH [4].

At optimum pH 8.0, about 95% of the imidazole ring is in deprotonated form; however, protonation of His137 is required for the reduction reaction. Ser116 assists protonation of His137 to drive the reduction reaction (Fig. 3A). A hydride is transferred from NADH causing the reduction of FHMPC to 4-pyridoxic acid with regeneration of NAD^+ (Fig. 3B). In our previous study, H137L mutation produced an inactive enzyme showing that this residue is crucial for catalysis of this enzyme [4]. Asn140, which is located near the nicotinamide ring, is likely involved in substrate anchoring. Mutation of ser116, Asn140 and Asn188 and crystallization of FHMPCDH with a substrate is currently underway to completely elucidate the reaction mechanism of this unique enzyme.

Acknowledgments

The authors would like to thank the staff of beamline BL26B1 of spring-8, Japan for their kind assistance during data collection. The authors would also like to thank Dennis Murphy from the United Graduate School of Agricultural Sciences, Ehime University for

checking English in this manuscript. This work was supported by Japan Society for the Promotion of Science (JSPS), Japan, grant number 22580052.

Appendix A. Supplementary data

Supplementary data associated with this article can be found, in the online version, at http://dx.doi.org/10.1016/j.bbrc.2014.11.028.

References

[1] R.W. Burg, V.W. Rodwell, E.E. Snell, Bacterial oxidation of vitamin B_6. II. Metabolites of pyridoxamine, J. Biol. Chem. 235 (1960) 1164–1169.
[2] B. Yuan, Y. Yoshikane, N. Yokochi, K. Ohnishi, T. Yagi, The nitrogen-fixing symbiotic bacterium *Mesorhizobium loti* has and expresses the gene encoding pyridoxine 4-oxidase involved in the degradation of vitamin B6, FEMS Microbiol. Lett. 234 (2004) 225–230.
[3] T. Nagase, A.N. Mugo, H.N. Chu, Y. Yoshikane, K. Ohnishi, T. Yagi, The mll6786 gene encodes a repressor protein controlling the degradation pathway for vitamin B_6 in *Mesorhizobium loti*, FEMS Microbiol. Lett. 329 (2012) 116–122.
[4] N. Yokochi, Y. Yoshikane, S. Matsumoto, M. Fujisawa, K. Ohnishi, T. Yagi, Gene identification and characterization of 5-formyl -3-hydroxy-2-methylpyridine 4-carboxylic acid 5-dehydrogenase, an NAD^+ dependent dismutase, J. Biochem. 145 (2009) 493–503.
[5] Y.C. Lee, M.J. Nelson, E.E. Snell, Enzymes of vitamin B_6 degradation. Purification and properties of isopyridoxal dehydrogenase and 5-formyl-3-hydroxy-2-methylpyridine 4-carboxylic acid dehydrogenase, J. Biol. Chem. 261 (1986) 15106–15111.
[6] X. He, G. Zhang, F. Blecha, S. Yang, Identity of heart and liver L-3-hydroxyacyl coenzyme A dehydrogenase, Biochem. Biophys. Acta 1437 (1999) 119–123.
[7] B.E. Noyes, B.A. Bradshaw, L-3-Hydroxyacyl coenzyme A dehydrogenase from pig heart muscle, J. Biol. Chem. 248 (1973) 3052–3059.
[8] M. El-Fakhri, B. Middleton, The existence of an inner-membrane-bound, long acyl-chain-specific 3-hydroxyacyl-CoA dehydrogenase in mammalian mitochondria, Biochem. Biophys. Acta 713 (1982) 270–279.
[9] D.K. Novikov, G.F. Vanhove, H. Carchon, S. Asselberghs, H.J. Eyssen, P.P.V. Veldhoven, G.P. Mannaerts, Peroxisomal β-oxidation. Purification of four novel 3-hydroxyacyl-CoA dehydrogenase from rat liver peroxisomes, J. Biol. Chem. 269 (1994) 27125–27135.
[10] J.J. Barycki, L.K. O'Brien, J.J. Birktoft, A.W. Strauss, L.J. Banaszak, Pig heart short chain L-3-hydroxyacyl-CoA dehydrogenase revisited: sequence analysis and crystal structure determination, Protein Sci. 8 (1999) 2010–2018.
[11] Y. Xu, H. Li, Y.-H. Jin, J. Fan, F. Sun, Dimerization interface of 3-hydroxyacyl-CoA dehydrogenase tunes the formation of its catalytic intermediate, PLoS One 9 (4) (2014) e95965.
[12] J.J. Barycki, L.K. O'Brien, J.M. Bratt, R. Zhang, R. Sanishvili, A.W. Strauss, L.J. Banaszak, Biochemical characterization and crystal structure determination of human heart short chain L-3-hydroxyacyl-CoA dehydrogenase provide insights into catalytic mechanism, Biochemistry 38 (1999) 5786–5798.
[13] J.J. Barycki, L.K. O'Brien, A.W. Strauss, L.J. Banaszak, Sequestration of the active site by interdomain shifting: crystallographic and spectroscopic evidence for distinct conformations of L-3-hydroxyacyl-CoA dehydrogenase, J. Biol. Chem. 275 (2000) 27186–27196.
[14] J.J. Barycki, L.K. O'Brien, A.W. Strauss, L.J. Banaszak, Glutamate 170 of human L-CoA dehydrogenase is required for proper orientation of the catalytic histidine and structural integrity of the enzyme, J. Biol. Chem. 276 (2001) 36718–36726.
[15] X.Y. He, S.Y. Yang, Histidine-450 is the catalytic residue of L-3-hydroxyacyl coenzyme A dehydrogenase associated with the large R-subunit of the multienzyme complex of fatty acid oxidation from *Escherichia coli*, Biochemistry 35 (1996) 9625–9630.
[16] X.Y. He, H. Deng, S.Y. Yang, Importance of the γ-carboxyl group of glutamate-462 of the large R-subunit for the catalytic function and the stability of the multienzyme complex of fatty acid oxidation from *Escherichia coli*, Biochemistry 36 (1997) 261–268.
[17] S. Ishikura, N. Usami, M. Araki, A. Hara, Structural and functional characterization of rabbit and human L-gulonate 3-dehydrogenase, J. Biochem. 137 (2005) 303–314.
[18] Y. Huanga, Z. Lua, N. Liua, Y. Chena, Identification of important residues in diketoreductase from *Acinetobacter baylyi* by molecular modeling and site-directed mutagenesis, Biochimie 94 (2012) 471–478.
[19] M. Lu, Y. Huang, M.A. White, X. Wu, N. Liu, X. Cheng, Y. Chen, Dual catalysis mode for the dicarbonyl reduction catalyzed by diketoreductase, Chem. Commun. 48 (2012) 11352–11354.
[20] G.T. Henehan, N.J. Oppenheimer, Horse liver alcohol dehydrogenase-catalyzed oxidation of aldehydes: dismutation precedes net production of reduced nicotinamide adenine dinucleotide, Biochemistry 32 (1993) 735–738.
[21] S. Svensson, A. Lundsjö, T. Cronholm, J-O. Höög, Aldehyde dismutase activity of human liver alcohol dehydrogenase, FEBS Lett. 394 (1996) 217–220.
[22] M.M. Bradford, A rapid and sensitive method for the quantitation of microgram quantities of protein utilizing the principle of protein–dye binding, Anal. Chem. 72 (1976) 248–254.
[23] A. Vagin, A. Teplyakov, Molecular replacement with MOLREP, Acta Crystallogr. D66 (2010) 22–25.
[24] M.D. Winn, C.C. Ballard, K.D. Cowtan, E.J. Dodson, P. Emsley, P.R. Evans, R.M. Keegan, E.B. Krissinel, A.G.W. Leslie, A. McCoy, S.J. McNicholas, G.N. Murshudov, N.S. Pannu, E.A. Potterton, H.R. Powell, R.J. Read, A. Vagin, K.S. Wilson, Overview of the CCP4 suite and current developments, Acta Crystallogr. D67 (2011) 235–242.
[25] G.N. Murshudov, A.A. Vagin, E.J. Dodson, Refinement of macromolecular structures by the maximum-likelihood method, Acta Crystallogr. D53 (1997) 240–255.
[26] P. Emsley, K. Cowtan, Coot: model-building tools for molecular graphics, Acta Crystallogr. D60 (2004) 2126–2132.
[27] P.D. Adams, R.W. Grosse-Kunstleve, L.-W. Hung, T.R. Ioerger, A.J. McCoy, N.W. Moriarty, R.J. Read, J.C. Sacchettini, N.K. Sauter, T.C. Terwilliger, PHENIX: building new software for automated crystallographic structure determination, Acta Crystallogr. D58 (2002) 1948–1954.
[28] R.A. Laskowski, M.W. MacArthur, D.S. Moss, J.M. Thornton, PROCHECK: a program to check the stereochemical quality of protein structures, J. Appl. Crystallogr. 26 (1993) 283–291.
[29] A.A. Vaguine, J. Richelle, S.J. Wodak, SFCHECK: a unified set of procedures for evaluating the quality of macromolecular structure-factor data and their agreement with the atomic model, Acta Crystallogr. D55 (1999) 191–205.
[30] Y. Chen, C. Chen, X. Wu, Dicarbonyl reduction by single enzyme for the preparation of chiral diols, Chem. Soc. Rev. 41 (2012) 1742–1753.
[31] Y. Asada, C. Kuroishi, Y. Ukita, R. Sumii, S. Endo, T. Matsunaga, A. Hara, N. Kunishima, Dimeric crystal structure of rabbit L-gulonate 3-dehydrogenase/λ-crystallin: insight into the catalytic mechanism, J. Mol. Biol. 401 (2010) 906–920.
[32] L. Holm, C. Sander, Protein structure comparison by alignment of distance matrices, J. Mol. Biol. 233 (1993) 123–138.
[33] E.-J. Kim, K.-J. Kim, Cloning, expression, purification, crystallization and X-ray crystallographic analysis of (S)-3-hydroxybutyryl-CoA dehydrogenase from *Clostridium butyricum*, Acta Crystallogr. F70 (2014) 485–488.
[34] P. Kasaragod, W. Schmitz, J.K. Hiltunen, R.K. Wierenga, The isomerase and hydratase reaction mechanism of the crotonase active site of the multifunctional enzyme (type-1), as deduced from structures of complexes with 3S-hydroxy-acyl-CoA, FEBS J. 280 (2013) 3160–3175.